

Tensile behavior of polyolefin composites: The effect of matrix parameters

Maria Guseva, Victor Gerasin, Boris Shklyaruk

A.V. Topchiev Institute of Petrochemical Synthesis, Russian Academy of Sciences, Leninskii Pr, 29, Moscow 119991, Russia
Correspondence to: M. Guseva (E-mail: guseva@ips.ac.ru)

ABSTRACT: Polyolefin composites were prepared from 14 PE matrices and three different mineral fillers (montmorillonite, palygorskite and glass microspheres) via melt compounding in an extruder. Mechanical properties of the obtained systems were analyzed with emphasis on elongation at break and conditions for ductile/brittle failure were determined. When filler content is raised beyond a certain “critical” value, tensile properties are dramatically altered and transition occurs from ductile behavior to brittle fracture. This transition is displayed by a well-defined “step” on the plot of strain at break versus concentration of particles. The value of “critical filler content” was found to depend mainly on level of crystallinity of a matrix while other parameters (chemical nature of filler particles, their size, shape and surface treatment) are less significant. “Critical filler content” will decrease with growth of crystallinity of a polymer and with highly crystalline HDPEs it is as low as 2–8 vol %. Otherwise, with noncrystallizing and low-crystalline polymers elongation at break decreases gradually with concentration of mineral particles and ductile type deformation is maintained at fairly large filler fractions. The results presented here will be useful for a proper selection of a matrix polymer in composites with mineral fillers. © 2016 Wiley Periodicals, Inc. *J. Appl. Polym. Sci.* **2016**, *133*, 43819.

KEYWORDS: composites; mechanical properties; morphology; polyolefins; structure–property relations

Received 1 July 2015; accepted 15 April 2016

DOI: 10.1002/app.43819

INTRODUCTION

Nowadays intensive research is carried out in the field of polymer composites. Reinforcements are used to reduce flammability, gas, and vapor permeability, to increase stiffness, dimension stability, wear, and corrosion resistance.^{1–4} On the other hand, addition of reinforcing particles to thermoplastic polymers leads to decrease in the elongation at break of the composites. This is an important drawback of filled polymers, since materials, easily broken under the effect of external load, cannot be applied in practice.

Mechanical performance of composites, which contain equal amount of the same filler, can be entirely different and is primarily controlled by the properties of matrix polymers. It was reported in publications,^{5–7} that composites with homogeneously deformable matrices behave in a fundamentally different manner than composites based on polymers exhibiting necking. In the former case, the elongation at break decreases monotonically with increasing filler content. In the latter case, an abrupt decrease in ultimate strain (embrittlement) occurs at some filler concentration, which was termed “critical”. Therefore, proper selection of a matrix for composite fabrication is a matter of great importance for end-use properties.

The main objective of the present study is to analyze the influence of matrix parameters on mechanical behavior of composites with emphasis on elongation at break. Polyethylene—a classical model polymer with simple chemical structure—was applied as a polymer binder in this work. There are many kinds of polyethylene (both commercial and synthesized in laboratories) which differ in molecular weight, content of side groups, their length, distribution and chemical composition. Therefore, to a first approximation, it was necessary to choose the parameter that would take into account all the features of polyethylene.

According to crystallization theory by Flory,⁸ side branches and comonomer units are normally expelled from polyethylene crystals during crystallization and reside in amorphous zones, except for short methyl groups which can enter lamellas. Longer branches are thought to be excluded from crystalline lattice, but some papers report their possible nonequilibrium entry into crystallites on very fast cooling of the melt.⁹

It was observed experimentally, that density and level of crystallinity decrease roughly linearly with increasing concentration of side branches (when branch type, length, and distribution are kept constant).^{10–12} Chemical species, length, and distribution of pendant groups along the polymer main chain also have an

Table I. Characteristics of PE Polymers Used as Matrices in the Study

N	Polymer type	Density (g/cm ³)	M _w	M _w /M _n	C _{cryst} (%)
PE-1	Ethylene-1-octene copolymer, 10% octene	0.890	39760	2.4	0
PE-2	Ethylene-vinyl acetate, 18% VA	0.935	72600	6.2	12
PE-3	LDPE «107-02K»	0.916	187000	4.5	23
PE-4	LDPE «Ch05»	0.917	139594	2.8	25
PE-5	bimodal PE «153-10K»	0.920	168678	10.3	27
PE-6	MDPE «Stam03»	0.931	81691	3.8	41
PE-7	Low-pressure PE «RA»	0.940	302100	8.9	42
PE-8	Low-pressure PE «BfK»	0.940	290700	7.9	43
PE-9	PE «PY-342»	0.945	398000	3.2	47
PE-10	PE «277»	0.949	58530	8.0	52
PE-11	PE «Host03»	0.951	63114	7.6	53
PE-12	Medium-pressure PE «I2»	0.958	68999	3.8	57
PE-13	Medium-pressure PE «I4.3»	0.960	65412	8.7	59
PE-14	PE «B150383»	0.963	50596	7.1	62

influence on density and degree of crystallinity. For linear (unbranched) polyethylenes it was reported that increase in weight-average molecular weight leads to decrease in density and degree of crystallinity.¹¹ Thus, density (or level of crystallinity which is linearly proportional to density^{13,14}) can be regarded as an integral criterion which encompasses other molecular characteristics, and can be used for comparison of different PE specimens.

Selecting polymers for this study, we tried to collect samples with various crystalline structure—from purely amorphous to high-crystalline, but we did not include into this range polymers with 100% crystallinity—PE monocrystals. Although these samples are of great fundamental interest, they are unlikely to be used as matrices in commercial composites. Density of PE samples used in this study ranges from 0.890 to 0.963 g/cm³, and degree of crystallinity—from 0 to 80%.

These polymers were compounded with three different minerals. Montmorillonite (MMT) is a rather cheap reinforcement, derived from bentonite clays. It is frequently used as filler for polymer materials since composites on its basis display a range of good performance properties—increased modulus, thermal stability, reduced flammability, gas and vapor adsorption, corrosion resistance.^{15,16} The main structural element of MMT is a silicate plate with the diameter from 50 to a few hundred nm and the thickness about 1 nm. Parallel silicate layers are arranged in crystallites—tactoids, which agglomerate to form primary clay particles with length up to 10 μm. Palygorskite (PLG) is another clay mineral which consists of silicate fibers with the length 600–1100 nm and diameter 5–15 nm.^{17,18} Particles of both MMT and PLG have high aspect ratios (more than 30). Unlike them, a third filler—glass microspheres (GS) with the mean diameter 20 μm—is isotropic. GS are traditionally used to obtain concentration dependencies of mechanical characteristics of polymer composites.^{19,20}

EXPERIMENTAL

Twelve PE polymers and two copolymers (ethylene-1-octene and ethylene-vinyl acetate) were used as matrices in the study (Table I). All the polymers were supplied by the polymer plants “Volzhskiy” and “Kazanorgsintez”, Russia.

Weight and number average molecular weights were obtained by means of gel permeation chromatography following conventional procedures. Densities ρ and degrees of crystallinity C_{cryst} were determined at 20 °C using hydrostatic weighting and wide-angle X-ray diffraction correspondingly. Since these values are known to depend on details of crystallization procedure, samples for these measurements were prepared by the same processing method—rapid plunging from the melt into ice water (quenching). It enables to make a meaningful comparison between different specimens.

The most important characteristics of mineral fillers are given in Table II. To improve thermodynamic compatibility between inorganic particles and organic matrices, montmorillonite (MMT), and palygorskite (PLG) were modified with a surfactant—dioctadecyldimethylammonium bromide (DODAB) using a procedure described in Ref. 21. Quantity of the modifier adsorbed onto the clay corresponded to 1.0 cation exchange capacity (CEC). Glass microspheres (GS) with the mean diameter 20 μm were used as received.

The molten polymers were blended with the fillers using a laboratory twin-screw extruder Haake MiniLab Rheomex CTW5 (Thermo Electron Corporation). The MiniLab is a micro-compounder for blending of small amounts of material (7 cm³), equipped with conical screws (5/14 mm in diameter and a length of 110 mm), an integrated backflow channel and an inert gas flush system. The temperature of the extruder was held the same in each zone (flush die, cycle flow channel, and barrel zones). Preliminary experiments were conducted to establish conditions under which filler particles are

Table II. Characteristics of Minerals Applied as Fillers in the Study

Filler	Code	Chemical formula	CEC (meq/100 g)	Density (g/cm ³)	Shape
Montmorillonite	MMT	[Na ⁺ × nH ₂ O] (Al ₃ Mg)Si ₈ O ₂₀ (OH) ₄	93	2.86	Platelets
Palygorskite	PLG	(Mg,Al) ₅ (Si ₈ O ₂₀)(OH) ₂ (H ₂ O) ₄ ·nH ₂ O	35	2.15	Fibers
Glass microspheres	GS	CaO·Na ₂ O·6SiO ₂	—	0.80	Spheres

CEC, cation exchange capacity.

dispersed rather uniformly in the matrix and thermal or mechanical destruction of polymers does not begin yet. Processing temperatures of the polymers were selected on the basis of their melting points and were 140 °C for PE-1 and PE-2, 150 °C for PE-3–PE-5, 160 °C for PE-6–PE-9, 170 °C for PE-10–PE-14. An inert gas flush system was used to prevent thermal degradation of matrix polymers. After blending, the extrudate was collected and used to prepare tensile test specimens. The composites were heated again up to their processing temperatures, compression molded at pressure of 0.5 MPa during 5 min and then rapidly quenched in ice water.

Mechanical tests were done on dog-bone specimens with dimensions of the working area 10 × 3 × 0.4 mm using a tensile testing machine Instron 1121. Tensile diagrams were recorded at ambient temperature and rate of drawing 50%/min. Our previous experiments showed that under these deformation conditions temperature of stretched polymers and composites does not rise and therefore the deformation process is close to isothermal.²² True stress–strain curves were not obtained, but nominal stress–strain plots are quite adequate for the present purpose. Structure of pristine and deformed polymers and composites was studied by means of AFM (Dimension Icon microscope), SEM (Jeol JSM-35C apparatus), and X-ray analysis (DRON-3 diffractometer).

DSC traces were recorded using a calorimeter DTAS-1300 (Russia) in the range from room temperature to 200 °C at a heating and cooling rate of 8 °C/min. Since all the specimens for DSC-measurements (the neat polymers and the composites) were prepared by the same processing method—rapid plunging from the melt into ice water, a rational comparison between the samples can be made based on the first run of heating. Polymer samples of 15 mg were heated in standard aluminum pans, the contribution of an empty pan was subtracted from each flow curve. The melt-

ing and crystallization temperatures were defined as maximum peaks of endotherms and exotherms, respectively.

Raman spectra were recorded at ambient temperature using an Ar⁺ laser source for excitation and a Triax monochromator and CCD detector (CCD 3500, Jobin Yvon, France) for signal detection and analysis.

RESULTS AND DISCUSSION

Distribution and Arrangement of Filler Particles in the Composites

Depending on the dispersion of clay, there exist three types of polymer–clay composites: intercalated, exfoliated and conventional.^{15,16} AFM micrographs show flat inclusions with the diameter 200–500 nm for composites with MMT (Figure 1) and needle-shaped inclusions with the length 200–800 nm for composites with PLG (Figure 2). Besides individual silicate particles, in both series of samples spherical or irregular-shaped agglomerates were detected which are also visible in optical microscope images. These aggregates consist of nondispersed clay tactoids/fibers and have the size up to 3–4 μm. Similar information about clay structure was obtained from SEM micrographs (Figure 3). These results suggest that the preparation method used in this work does not enable to divide all the silicate particles in the composite into nanosized sheets or fibers.

Incomplete dispersion or aggregation of nanoparticles during preparation or usage of materials is a common problem for many composite systems,²³ it leads to significant difference between expected structure predicted by composite theories and real structure.

Rigid filler particles, when incorporated into a polymer matrix, are known to act in two ways.²⁴ On the one hand, they bear a significant part of the applied load and thus improve mechanical

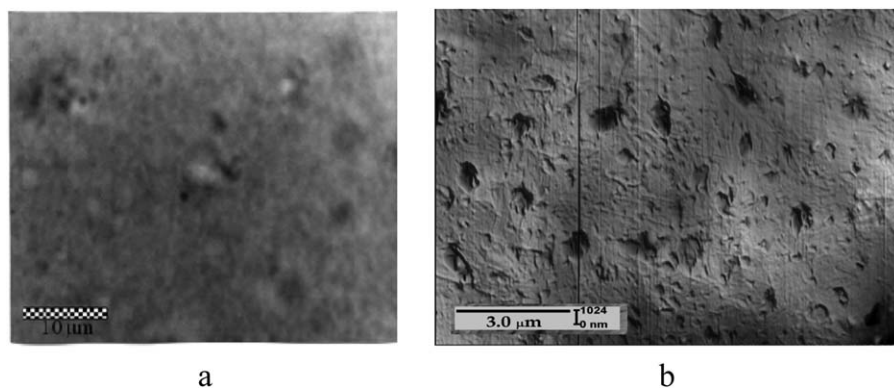


Figure 1. Optical (a) and AFM image (b) of the composite PE-7/5 wt % MMT.

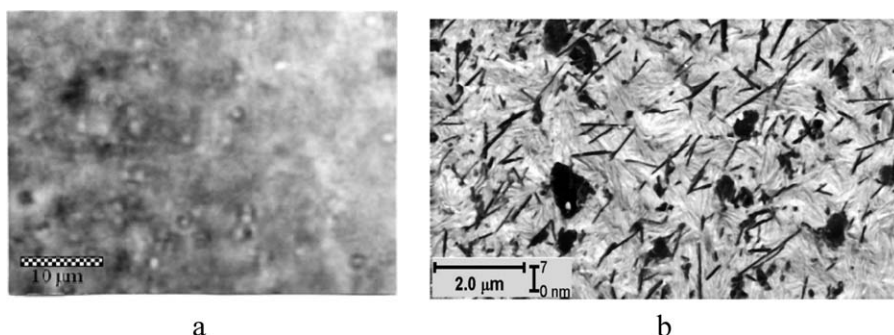


Figure 2. Optical (a) and AFM image (b) of the composite PE-7/5 wt % PLG.

characteristics of the system. On the other hand, they trigger processes of internal damage which cause weakening of the material. If inherent strength of inclusions is rather low, they are easily destroyed under deformation which is often the case for composites with natural fibers.²⁵ Stronger particles tend to detach from the matrix and become centers of voids formation and growth.

According to the model by Gent,²⁶ the stress necessary to initiate debonding σ_d depends on size of inclusions r in the following way: $\sigma_d^2 \sim 1/r$. A similar relation between debonding stress and radius of the particle was derived in publication.²⁷ As follows from the above equation, the larger particles detach from the binder at lower stresses than the smaller ones. Therefore, macroscopic mechanical properties of composites with particles of different dimensions are controlled by the biggest inclusions. In connection with the foregoing, MMT and PLG-based materials can be classified as conventional microcomposites as well as composites of the model series with glass microspheres.

Morphology of PE-Matrix in the Composites

It is known, that incorporation of mineral fillers into crystalline polymers, even in small concentrations, can affect significantly

crystalline structure of the matrices. It was established that MMT particles act as nucleating agents for PETE,²⁸ PP,²⁹ and PA.³⁰

Morphology of PE-matrix in the investigated composites was studied by means of X-ray analysis, DSC, and Raman spectroscopy and the obtained data were compared with those for the neat PEs. In the X-ray patterns of composites with MMT (Figure 4) in the low-angle region $2\theta < 8^\circ$ two new Bragg's maxima were revealed corresponding to first- and second-order basal reflections (001) of the clay sheets.^{15,16} Diffractograms of PE-PLG composites contain a maximum at $2\theta = 8.3^\circ$, relating to scattering of palygorskite fibers.¹⁸ Examination of the main PE maxima (110) and (200) ($2\theta = 21.4^\circ$ and 23.7°) showed that they retain their shape and angular position in the filled samples, while their intensity diminishes because of decrease in PE content in the systems.

DSC curves of the samples under study are presented in Figure 5. No additional endothermic or exothermic peaks were revealed for the composites. The heating and cooling curves of all specimens have only one well-defined maximum, which corresponds to melting or crystallization of PE orthorhombic crystals. In the presence of fillers, shape and location of this maximum on the temperature scale is the same as in the neat PE (within the measuring accuracy of the calorimeter), and its area is smaller since PE concentration in the filled systems is below 100%.

It is known that Raman spectra can provide information about both crystalline and amorphous areas of polymers. It is important to note, that clay minerals yield a featureless Raman spectrum, which does not mask signals of polymers. The spectra and characteristics calculated from them are given in Figure 6 and Table III, respectively (a more detailed study of the Raman spectra is described in Ref. 31). The Raman bands of the composite are very similar in shape and position to those of the neat PE. Consequently, PE and PE matrix of the composites have very close values of crystallinity level, size of crystallites and concentration of *trans*- and *gauche*-conformers in the amorphous areas.

Summarizing the data in "Morphology of PE Matrix in the Composites" we can state, that structural parameters of PE (type and dimensions of crystal lattice, size of crystallites, degree of crystallinity, distribution of conformers in amorphous regions) are not affected by presence of MMT and PLG and their content in the material. This may be due to high

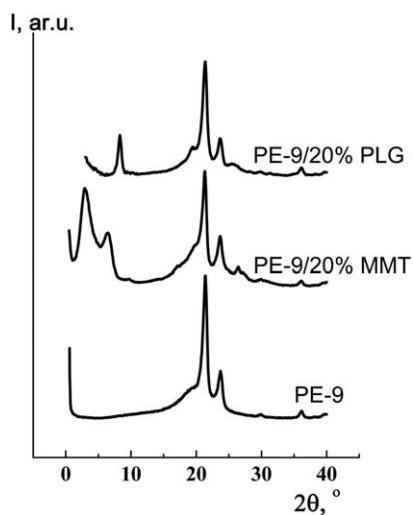


Figure 3. SEM image of the composite PE-2/3% MMT stretched up to break. The arrows indicate the direction of the deformation.

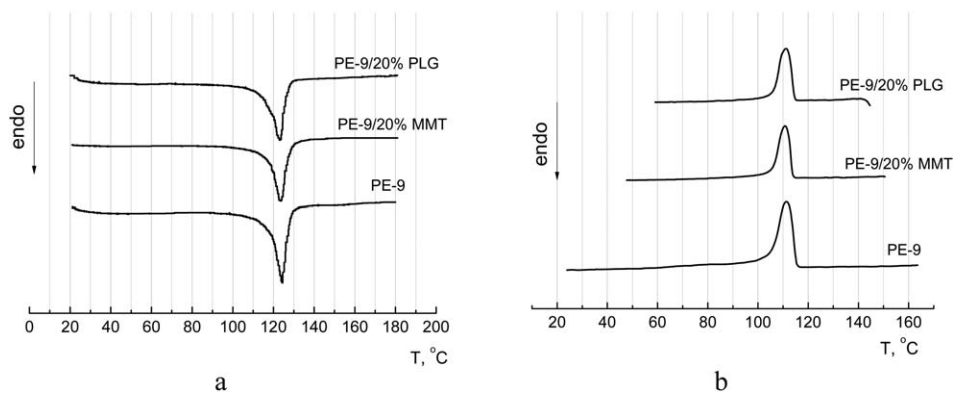


Figure 4. X-ray patterns of the neat PE-9 and its composites with montmorillonite and palygorskite.

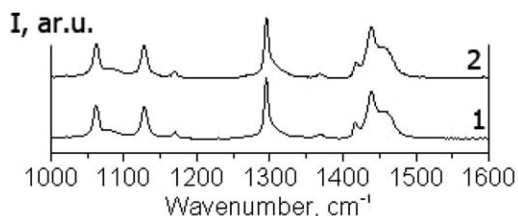


Figure 5. DSC-traces of the neat PE-9 and its composites with montmorillonite and palygorskite, heating (a), and cooling (b) curves.

crystallization rate of PE,³² when presence of filler surface do not have a significant impact on crystallization kinetics of PE macromolecules. As a consequence, changes in mechanical behavior of filled PEs are not related to changes in their crystalline structure.

Analysis of mechanical properties of the composites showed that different kinds of PE «respond» to incorporation of the same filler in a different way, while filled polymers with close values of crystallinity/density proved to have similar deformation features. As a result, 14 series of the composites were divided into 4 groups.

Tensile Properties of Composites of Groups 1 and 2

Group 1 comprises copolymers ethylene-1-octene (PE-1) and ethylene-vinyl acetate (PE-2). PE-1 is a fully amorphous polymer whose tensile habits are similar to those of rubbers. PE-1

deforms uniformly, without necking, stress increases monotonously with elongation [Figure 7(a)].

Although PE-2 has a low fraction of crystalline phase (12% according to X-ray data), small imperfect crystalline regions act rather as crosslinks for molecules in the prevailing amorphous component, therefore tensile behavior of this polymer also resembles deformation of crosslinked rubber systems [Figure 7(a)].

When filler is added to the polymer, the actual shape of the tensile diagram remains unchanged, but the curve becomes shorter, and values of ultimate strength and elongation tend to decrease compared to the neat polymer [Figure 7(b)]. In this series of samples strain at break decreases smoothly, without quick transition to brittle fracture [Figure 8(a)]. Such dependence of elongation on reinforcement content is typical for rubber-based composites.

Premature failure of filled polymers is caused by formation and growth of pores around filler particles. The role of voids in deformation process and failure mechanism of composites was investigated in Refs. 33–35 two types of pores were detected—oval and rhombic-like. Oval cavitations emerge around relatively small inclusions. At low concentrations of filler, when stress fields around neighboring particles do not interact, dimensions of oval pores remain stable for a long time. The voids begin to grow and coalesce at the region of strain hardening. As a consequence, ultimate elongation of the filled polymer

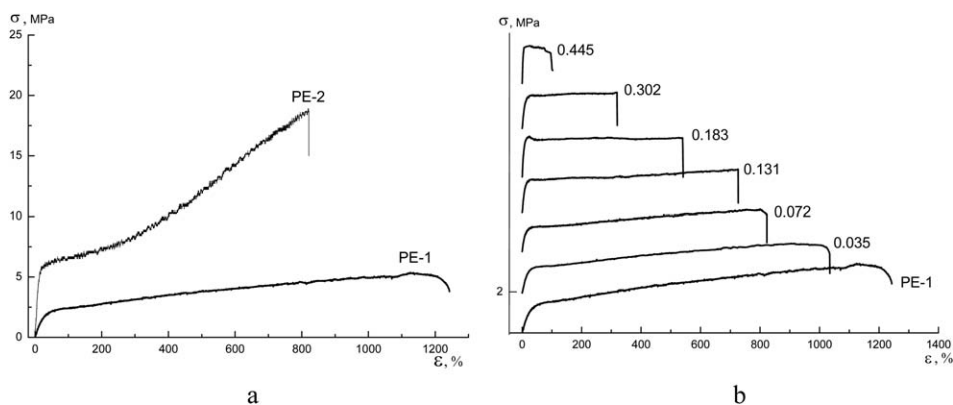


Figure 6. The Raman spectra of the neat PE-4 (a) and the composite PE-4/5 wt % MMT (b).

Table III. Characteristics Derived from the Raman Spectra

Sample	C_{cryst} (%)	C_{trans} (%)	C_{gauche} (%)
PE-4	27	62	35
PE-4/5 wt % MMT	25	65	35

C_{cryst} , content of the orthorhombic PE crystallites.

C_{trans} , total content of CH_2 chains in *trans*-conformation.

C_{gauche} , content of *gauche*- conformers in noncrystalline areas.

is only a little smaller than that of the neat polymer. Rhombic-shaped pores are formed around large inclusions. In the tip of such a void stress concentration rises significantly, it causes the pore to quickly propagate through the whole cross-section of the sample and leads to fracture at small strains.

It was established that for every polymer there exists a critical size of particles D_c which initiate formation of rhombic cavitations, for LDPE it is $\approx 400 \mu\text{m}$.³³ All the fillers used in this study have much smaller dimensions, therefore oval pores were observed around the inclusions in SEM micrographs of deformed composites (Figure 3). At relatively small concentrations voids are located far from each other and almost do not interact. They begin to grow and merge at later stages of deformation therefore strain at break of composites with moderate filler contents is not very different from that of the neat polymer.

When reinforcement fraction is increased, the thickness of polymer interlayer between neighboring rigid particles decreases and pores begin to interact and combine at earlier stages of deformation which leads to significant reduction in ultimate elongation of highly filled systems.

Starting from degree of crystallinity $C_{\text{cryst}} \approx 20\%$, crystalline phase begins to play a significant role in mechanical behavior of polymers. Low-density polymers PE-3, PE-4, and PE-5, which belong to group 2, deform with a weakly pronounced («diffuse») neck. Tensile diagrams of this series of samples show a wide and flat yield maximum followed by a horizontal portion («yield plateau», corresponding to propagation of neck along the sample's length) and then by a strain hardening region [Figure 9(a)].

As well as neat low-density polyethylenes, composites on their basis display a weakly pronounced neck under drawing. At

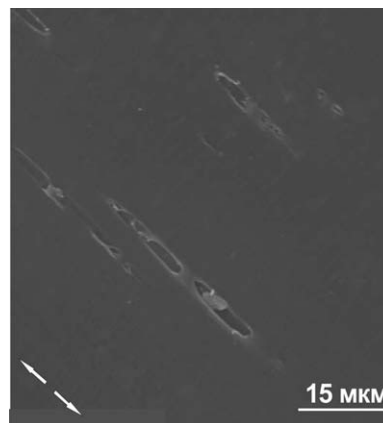


Figure 8. Elongation at break as a function of MMT content for group 1 (a) and 2 (b).

moderate concentrations of mineral particles the neck propagates along the whole gauge length of the composite, and the region of strain hardening tends to reduce, which leads to lower values of ultimate elongation and strength compared to the neat LDPEs [Figure 9(b)].

At a certain filler fraction ($\varphi = 0.2, 0.34, \text{ and } 0.16$ for PE-3, PE-4, and PE-5, respectively), the composite's strength goes down to the stress of neck's propagation. In this case the neck, which is being formed, becomes unstable and failure may occur at any strain at «the yield plateau». At larger filler contents, the composites fracture at the onset of necking. In this series of composites dependence of ultimate elongation on filler fraction is not quite monotonous, when the neck becomes unstable, the rate of strain decreasing somewhat increases [Figure 7(b)].

Another important matter of investigation is influence of filler type on tensile behavior of composite systems. Plots of ultimate elongation versus filler volume fraction are presented in Figure 10 for three series of composites—with MMT, PLG, and GS (matrix polymer—PE-3). One can see, that at equal filler concentrations, composites with different fillers fracture at similar strains. The reinforcements used in this work have different chemical nature, shape, and size of particles. The obtained data lead to the assumption that these characteristics do not affect significantly ultimate properties of composites and they are primarily determined by matrix parameters.

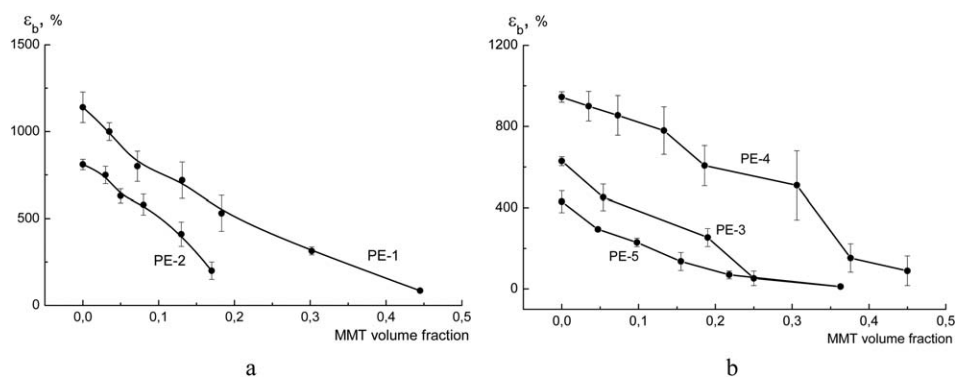


Figure 7. Stress–strain curves of neat PE-1 and PE-2 (a) and PE-1/MMT composites (b). Figures near the curves are MMT volume fractions.

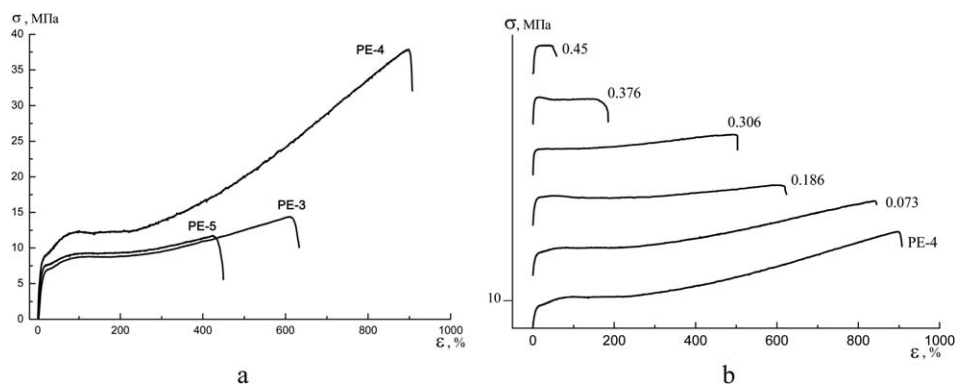


Figure 9. Stress–strain curves of neat PE-3, PE-4, and PE-5 (a) and PE-4/MMT composites (b). Figures near the curves are MMT volume fractions.

Composites systems under study were prepared without addition of compatibilizers. Maleated polyolefins were used to improve interfacial adhesion between nonpolar PE and polar MMT in publication.³⁶ It was established that the values of ultimate elongation of systems with and without the compatibilizers are close, which confirms the assumption about domineering influence of matrix polymer properties.

Tensile Properties of Composites of Groups 3 and 4

Polymers which refer to group 3 have approximately equal amounts of crystalline and amorphous components ($C_{\text{cryst}} \approx 40\text{--}50\%$). When level of crystallinity increases, the yield point on the tensile diagrams becomes “sharper” and well-defined and shifts to lower strains ($\varepsilon \approx 20\%$) [Figure 11(a)]. After passing of the upper yield point, the nominal stress drops by $\Delta\sigma = 2.2\text{--}4.6$ MPa. Correspondingly, the neck is well visible on the working area of the polymer and has distinct boundaries between oriented and isotropic zones.

Evolution of stress–strain curves with increasing filler content is presented in Figure 11(b). Formation of pores around the inclusions leads to reduction in the working cross-section of the filled polymer, and, as a consequence, to reduction in strength. While the strength remains bigger than the lower yield stress,

the neck propagates in a steady fashion and the composite fracture at the region of strain hardening. When the strength decreases down to the lower yield stress, neck’s propagation can be interrupted. In this case a big deviation in values of ultimate elongation is observed. When filler fraction is further increased, failure of composites occurs at the onset of necking, usually at the upper yield stress.

In connection with the foregoing, the plot of ultimate elongation versus filler volume fraction $\varepsilon_b(\varphi)$ has a step-like character [Figure 12]. The height of the step is approximately equal to the length of “yield plateau” on the tensile diagram. As stated above, filler content at which transition between ductile and brittle deformation takes place, is termed “critical” φ_{crit} .^{5,6} Typical values of φ_{crit} in this group of polymers were found to lie in the range 0.2–0.4 (Table IV).

No significant difference in φ_{crit} was detected among three series of composites—with MMT, PLG, and GB. It means that tensile properties of composites are primarily related to parameters of matrix polymers (provided that size of inclusions is smaller than critical D_c), while shape of particles, their chemical nature, interfacial adhesion are factors of less significance.

A decline, similar to a step, is also visible on plots of $\varepsilon_b(\varphi)$ for composites of group 2 [Figure 7(b)]. Since in this series, length of “the yield plateau” is not large and yield maximum is wide and flat, the step is not distinct and transition between ductile and brittle deformation is not so well-pronounced as in polymers with higher degree of crystallinity. Therefore, deformation type of group 2 can be regarded as intermediate between groups 1 and 3.

Group 4 comprises polyethylenes with the highest density and degree of crystallinity ($C_{\text{cryst}} > 50\%$). Among the studied polymers these samples also display the highest values of ultimate elongation $\varepsilon_b \approx 1500\text{--}2300\%$ [Figures 12 and 13(a)]. Stress–strain curves show a well-shaped yield maximum, after which the nominal stress drops by $\Delta\sigma = 7\text{--}11$ MPa. In the region of strain hardening slope of the curve is substantially smaller compared to polymers of the previous group. As a result, strength of filled HDPEs quickly decreases down to the value of lower yield stress, and deformability of composites reduces to a few %. Transition between ductile and brittle deformation occurs at filler volume fractions $\varphi < 0.1$ (Table IV).

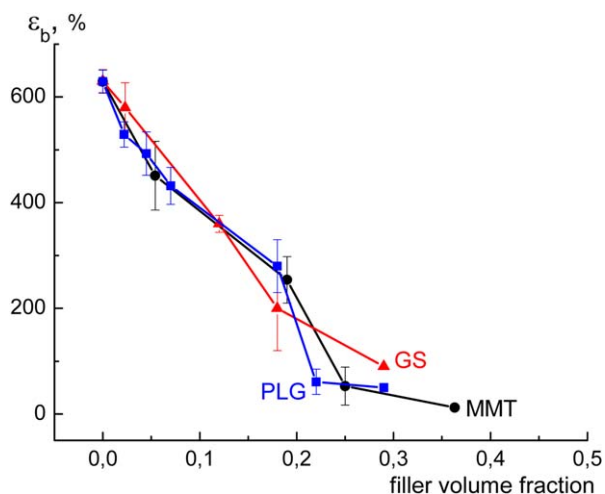


Figure 10. Elongation at break as a function of filler content for PE-3 composites with MMT, PLG, and GS. [Color figure can be viewed in the online issue, which is available at wileyonlinelibrary.com.]

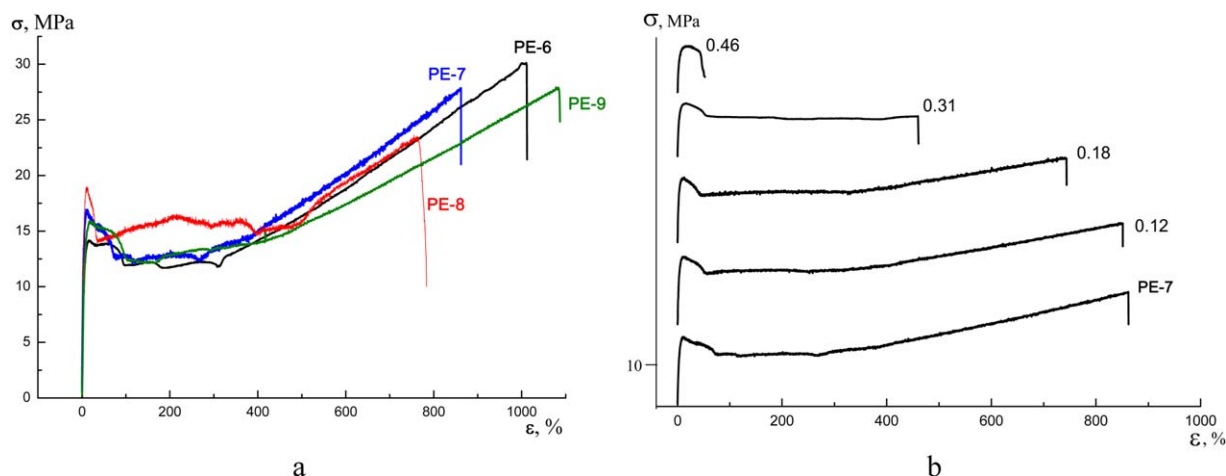


Figure 11. Stress–strain curves of neat PE-6, PE-7, PE-8, and PE-9 (a) and PE-7/MMT composites (b). Figures near the curves are MMT volume fractions. [Color figure can be viewed in the online issue, which is available at wileyonlinelibrary.com.]

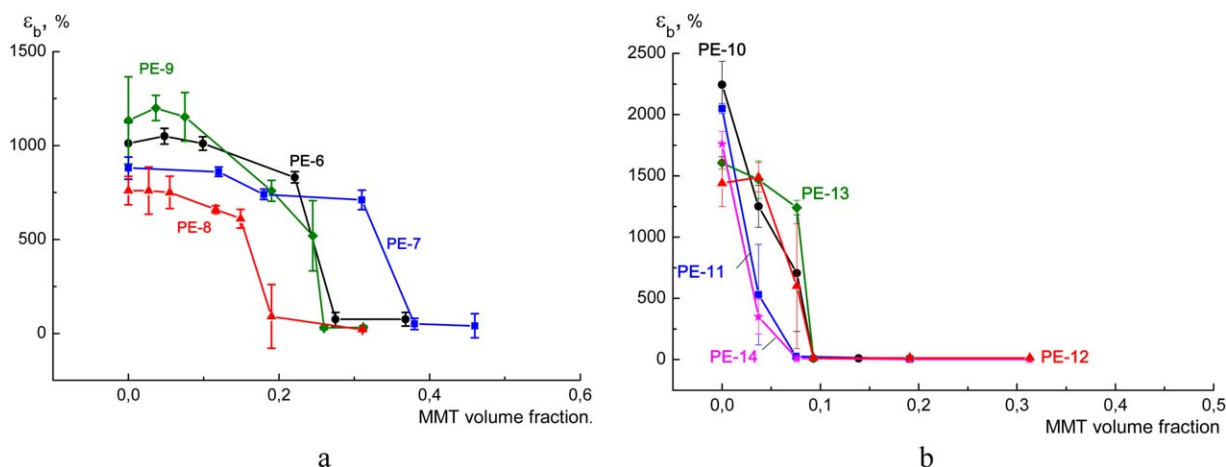


Figure 12. Elongation at break as a function of MMT content for groups 3 (a) and 4 (b). [Color figure can be viewed in the online issue, which is available at wileyonlinelibrary.com.]

Influence of Crystalline Structure on Deformation Behavior

It is evident, that differences between groups 1 and 4 are related to different morphology of matrix PEs, mainly to changing

Table IV. Critical Filler Content for Medium and High-Density Polyethylenes

Polymer	φ_{crit} , volume fraction		
	MMT	PLG	GS
PE-6	0.27	—	—
PE-7	0.38	—	—
PE-8	0.19	—	—
PE-9	0.25	0.22	0.27
PE-10	0.037	0.034	0.03
PE-11	0.037	—	—
PE-12	0.076	—	—
PE-13	0.08	—	—
PE-14	0.027	0.022	0.022

crystallinity. X-ray analysis was used to study crystalline structure of the polymers used as matrices. Diffractograms show that with increasing density, Bragg's maxima (110) and (200), corresponding to scattering of crystalline regions, become higher and narrower (Figure 14) (the scattering volume was kept constant in these measurements). X-ray patterns were used to calculate unit cell parameters, dimensions of crystallites in different crystallographic directions, packing density of molecules in crystallites, and total content of crystalline phase (Table V). It was discovered, that not only total value of crystallinity is different among LDPE, MDPE and HDPE, but the whole structure of crystalline regions. The largest crystallites with the densest molecular packing are formed in HDPE, and small imperfect crystallites with a loose packing—in LDPE.

Another step was changing of crystallinity of PE samples. DSC was applied to determine temperature of maximal crystallization rate and the polymers were annealed at this temperature for 3 h. As a consequence, level of crystallinity increased to about 30% for LDPE, 60%—for MDPE and 80%—for HDPE. Alongside the growth of total crystallinity content, dimensions of

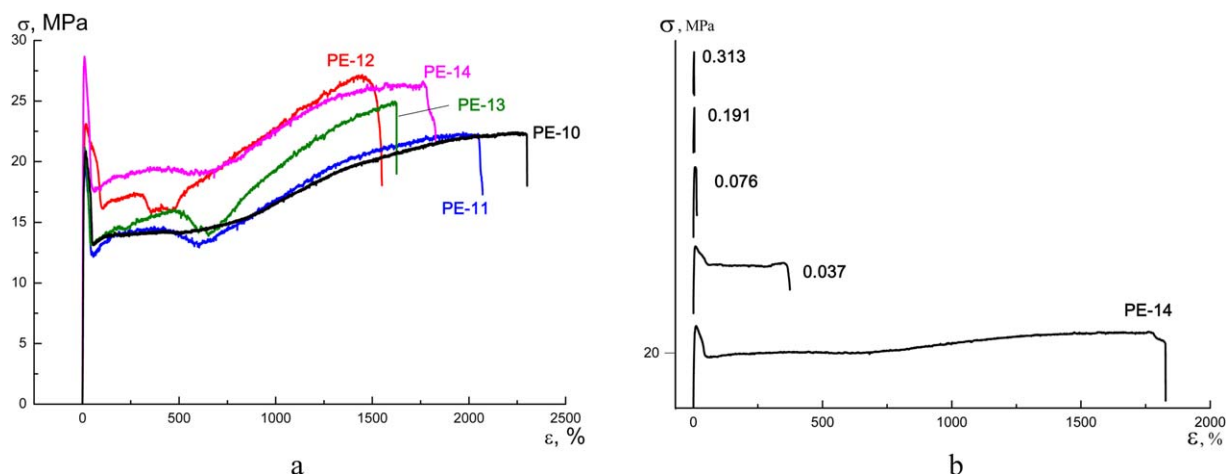


Figure 13. Stress–strain curves of neat PE-10, PE-11, PE-12, PE-13, and PE-14 (a) and PE-14/MMT composites (b). Figures near the curves are MMT volume fractions. [Color figure can be viewed in the online issue, which is available at wileyonlinelibrary.com.]

crystallites, and their packing density also increased. On the whole, crystalline structure of all the samples became more perfect due to isothermal crystallization.

Mechanical tests revealed that for LDPE and MDPE annealing leads to increase in initial modulus, upper and lower yield stresses, while strength and strain at break remain nearly unchanged (the tensile diagrams are not shown to save space).

For HDPE, larger fraction of crystalline component also leads to higher values of modulus and yield stress, but simultaneously it causes complete losing of ductile properties—strain at break drops to 8–10% (Figure 15). In this respect, mechanical properties of annealed neat polymers resemble those of composites when filler concentration exceeds a critical value. It is apparent that in both cases the reason for premature failure is decreasing

in amorphous content below a certain level. Flexible polymer chains, located outside crystal lattice, can easily change their conformation under the effect of external load and transfer mechanical energy to other chains, which helps to relieve stress concentration around inclusions and polymer crystallites. If number of molecules in amorphous interlayers is too small, mechanism of stress relaxation becomes impossible. In this case in regions of the highest stress concentration fracture begins which gives rise to formation of pores and sample's failure at low strains.

It becomes clear from the obtained results that for ductile type deformation of neat and filled polymers it is necessary that they contain sufficient amount of flexible amorphous component. According to our data, for PE samples such content of amorphous phase is about 20–30%. Strictly speaking, it would be physically more correct to introduce the term “critical” content of amorphous phase instead of “critical” filler content. Since it is amorphous interlayer, which provides mechanism of stress relaxation and maintains plastic deformation. But in practice, during processing and use of composites, it is more convenient to deal with concentration of filler than to calculate relative content of amorphous component in a complex composite system.

According to the “composite theory” of semicrystalline polymers,¹¹ polymer crystallites can be regarded as filler particles and surrounding amorphous component—as a binder. In this connection specimens of HDPE can be considered as composite systems in which filler concentration is close to “critical”. When real filler particles are incorporated into such polymers, total amount of rigid component increases more, while relative content of amorphous phase decreases below a threshold value. This leads to transition from ductile to brittle fracture at small concentrations of filler.

It was already noted, that in the systems available for this study, crystalline structure of PE is not affected by presence of inclusions. However, if a filler produces nucleating effect on a matrix polymer, values of “critical” filler fraction will be lower compared to systems with “inert” fillers.

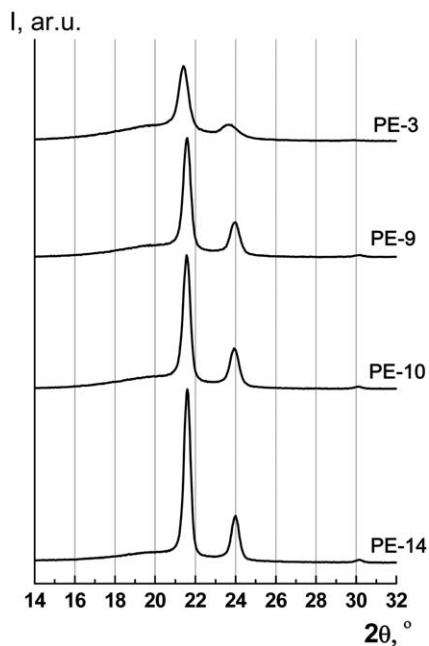


Figure 14. X-ray patterns of PE-3, PE-9, PE-10, and PE-14.

Table V. Crystalline Structure of Quenched and Annealed Polymers Determined by X-ray Analysis

Polymer		a (nm)	b (nm)	c (nm)	L ₁₁₀ (nm)	L ₂₀₀ (nm)	L ₀₂₀ (nm)	L ₀₀₂ (nm)	C _{cryst} (%)	ρ (g/cm ³)
PE-3	Quenched	0.751	0.496	0.253	14.5	8.5	10.0	—	23	0.988
	Annealed	0.743	0.493	0.253	15.0	10.0	15.0	—	28	1.005
PE-9	Quenched	0.743	0.494	0.254	19.5	15.0	16.0	7.5	47	0.999
	Annealed	0.740	0.494	0.254	22.5	20.0	19.0	8.0	58	1.003
PE-10	Quenched	0.743	0.494	0.254	22.0	18.5	17.0	8.0	52	0.999
	Annealed	0.739	0.492	0.254	23.5	21.5	17.0	9.0	75	1.009
PE-14	Quenched	0.742	0.494	0.254	22.0	18.5	16.5	8.0	62	1.000
	Annealed	0.739	0.493	0.254	24.0	22.0	18.0	9.0	80	1.007

a, b, c, unit cell parameters.

L₁₁₀, L₂₀₀, L₀₂₀, L₀₀₂, dimensions of crystallites in different crystallographic directions.

C_{cryst}, degree of crystallinity.

ρ, density of crystalline regions.

In contrast to HDPEs, noncrystallizing ethylene copolymers and low crystalline LDPEs display ductile deformation even at fairly large filler concentrations, therefore this group of polymers can be used for preparation of highly filled composite systems.

CONCLUSIONS

Polyethylenes with crystallinity 0–80% were blended with three different fillers (montmorillonite, palygorskite and glass spheres) and mechanical behavior of the obtained composites was investigated.

It was revealed that plots of ultimate elongation versus filler content can be of two types: (1) a monotonously decreasing curve; (2) a curve with a “step”, with separates regions of ductile and brittle fracture. The first type is observed in composites based on completely amorphous PE copolymers and polymers with very low degree of crystallinity. The second type is typical for filled polymers which contain fairly large portion of crystallites and exhibit necking under tensile deformation (MDPE and HDPE). In composites with low-crystalline LDPEs, fracture mode is transitional between types and 2 (a poorly shaped “step”).

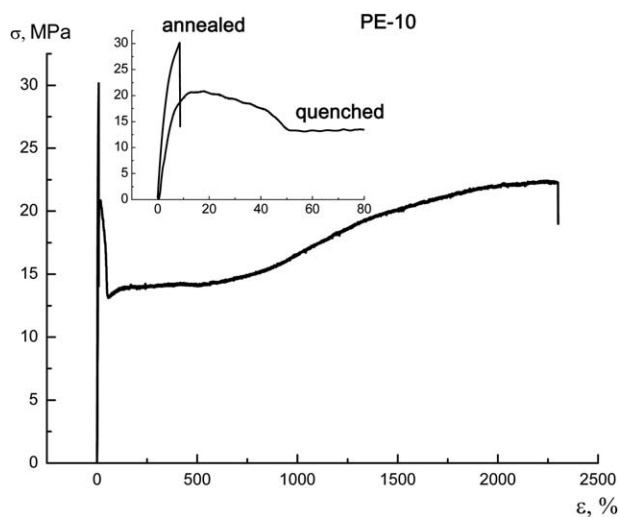


Figure 15. Stress–strain curves of quenched and annealed PE-10.

Position of the “step” on the plot of ultimate elongation versus filler fraction $\varepsilon(\varphi)$ determines critical concentration φ_{crit} at which ductile deformation is replaced by brittle fracture. The value of φ_{crit} was found to decrease with growth of crystallinity of a matrix polymer. Typical values of φ_{crit} are 0.2–0.4 vol. fraction for MDPEs and less than 0.1 vol. fraction for HDPEs.

It was established that necessary condition for ductile deformation of neat and filled polymers is sufficient content of flexible amorphous component which enables mechanism of stress transfer and relaxation.

ACKNOWLEDGMENTS

The studies were supported by grant No.15-03-08483 of the fund “Russian Foundation for Basic Research”.

REFERENCES

- Landel, R. F.; Nielsen, L. E. *Mechanical Properties of Polymers and Composites*; CRC Press: Boca Raton, **1993**.
- Xanthos, M. *Functional Fillers for Plastics*; John Wiley and Sons: New York, **2010**.
- Kozlov, G. V.; Mikitaev, A. K.; Zaikov, G. E. *Polymer and Composites: Theory and Practical Applications*; Nova Science Publishers, Inc.: New York, **2011**.
- Moczo, J.; Pukanszky, B. *J. Indus. Eng. Chem.* **2008**, *14*, 535.
- Bazhenov, S.; Li, J. X.; Hiltner, A.; Baer, E. *J. Appl. Polym. Sci.* **1994**, *52*, 243.
- Bazhenov, S. *Polym. Eng. Sci.* **1995**, *35*, 253.
- Bazhenov, S. L.; Grinev, V. G.; Kudina, O. I.; Novokshonova, L. A. *Polym. Sci. Ser. A* **2010**, *52*, 549.
- Flory, P. J. *Trans. Farad. Soc.* **1955**, *51*, 848.
- Hay, J. N.; Zhou, X. Q. *Polymer* **1993**, *34*, 1002.
- Peacock, A. J.; Mandelkern, L. J. *J. Polym. Sci. B: Polym. Phys.* **1990**, *28*, 1917.
- Popli, R.; Mandelkern, L. J. *J. Polym. Sci. B: Polym. Phys.* **1987**, *25*, 441.

12. Butler, M. F.; Donald, A. M.; Ryan, A. *J. Polym.* **1997**, *38*, 5521.
13. Selikhova, V. I.; Zubov, Y. A.; Bakeyev, N. F.; Belov, G. P. *Polym. Sci. U.S.S.R.* **1977**, *19*, 879.
14. Paricaud, P.; Galindo, A.; Jackson, G. *Indus. Eng. Chem. Res.* **2004**, *43*, 6871.
15. Alexandre, M.; Dubois, P. *Mater. Sci. Eng.* **2000**, *28*, 1.
16. Ray, S. S.; Okamoto, M. *Prog. Polym. Sci.* **2003**, *28*, 1539.
17. Chryssikos, G. D.; Gionis, V. V. *Am. Miner.* **2009**, *94*, 200.
18. Nasedkin, V. V.; Boeva, N. M.; Garbuzova, I. A.; Kovalchuk, M. V.; Vasiliev, A. L. *Crystallogr. Rep.* **2009**, *54*, 884.
19. Dubnikova, I. L.; Kedrina, N. F.; Solov'eva, A. B.; Timofeeva, V. A.; Erina, N. A.; Zarkhina, T. S.; Rozhkova, N. N. *Polym. Sci. Ser. A* **2003**, *45*, 281.
20. Ponomareva, N. R.; Goncharuk, G. P.; Grigor', E.; Yu, A.; Obolonkova, E. S.; Serenko, O. A. *Russ. J. Appl. Chem.* **2009**, *82*, 1472.
21. Gerasin, V. A.; Bakhov, F. N.; Merekalova, N. D.; Korolev, Y. M.; Fischer, H. R.; Antipov, E. M. *Polym. Sci. Ser. A* **2005**, *47*, 954.
22. Guseva, M. A.; Gerasin, V. A.; Garishin, O. K.; Plekhov, O. A.; Pawlak, A. *Polymer* **2015**, *56*, 416.
23. Ozerin, A. N. Nanoparticles in a Polymer Matrix. Present-Day Challenges; Proceedings of the 6th Kargin Conference "Polymers 2014", Moscow, Russia, January 27–31, **2014**, Vol. 1, p 246.
24. Garishin, O. K.; Gerasin, V. A.; Guseva, M. A. *Polym. Sci. Ser. A* **2011**, *53*, 1187.
25. Renner, K.; Moczo, J.; Pukanszky, B.; Suba, P. *Compos. Sci. Technol.* **2010**, *70*, 1141.
26. Gent, A. N. *Rubber Chem. Technol.* **1983**, *56*, 1011.
27. Pukanszky, B.; Voros, G. *Compos. Interfaces* **1993**, *1*, 411.
28. Harkin-Jones, E.; Figiel, L.; Spencer, P.; Abu-Zurayk, R.; Al-Shabib, W.; Chan, V.; Rajeev, R.; Soon, K.; Buckley, P.; Sweeney, J.; Menary, G.; Armstrong, C.; Assender, H.; Coates, P.; Dunne, F.; McNally, T.; Martin, P. *Plast. Rubber Compos.* **2008**, *37*, 113.
29. Antipov, E. M.; Barannikov, A. A.; Gerasin, V. A.; Shklyaruk, B. F.; Tsalamashvili, L. A.; Razumovskaya, I. V. *Polym. Sci. Ser. A* **2003**, *45*, 1140.
30. Fornes, T. D.; Paul, D. R. *Polymer* **2003**, *44*, 3945.
31. Sagitova, E. A.; Prokhorov, K. A.; Nikolaeva, G. Y.; Pashinin, P. P.; Gerasin, V. A.; Guseva, M. A.; Antipov, E. M. *Laser Phys.* **2008**, *18*, 868.
32. Krevelen, D. W.; Hoftyzer, P. J. Properties of Polymers: Correlations with Chemical Structure; Elsevier Publishing Company: Amsterdam, **1972**.
33. Serenko, O. A.; Bazhenov, S. I.; Nasrullaev, I. N.; Berlin, A. A. *Polym. Sci. Ser. A* **2005**, *47*, 49.
34. Ponomareva, N. R. Structural-Mechanical Features of Deformation Behavior of the Composite Materials Based on Polyolefins and Mineral Particles; Ph.D. Thesis, Moscow Pedagogical State University, **2010** [in Russian].
35. Ponomareva, N. R.; Desyatkov, A. V.; Goncharuk, G. P.; Obolonkova, E. S.; Budnitskiy, Y. M.; Serenko, O. A. *Materi- alovedenie* **2009**, *8*, 52 [in Russian].
36. Stoeffler, K.; Lafleur, P.; Florence, P.; Bureau, M.; Denault, J. *J. Compos. A* **2011**, *42*, 916.